ADVANCED APPROACHES TO THE CL-20/HMX COCRYSTAL

Dirk Herrmannsdörfer, Michael Herrmann and Thomas Heintz

Fraunhofer-Institut für Chemische Technologie ICT, Pfinztal Germany

e-mail to dirk.herrmannsdoerfer@ict.fraunhofer.de

ABSTRACT

Understanding the kinetic and thermodynamic of the formation of the 2:1 cocrystal of CL-20 and HMX is a key factor to optimize crystallization procedures in regard to time and material efficiency as well as crystal purity. Here we describe the influence of reaction conditions of Liquid Assisted Grinding (LAG) of HMX and CL-20 in 2-propanol on the reaction time and crystal quality of the 2:1 cocrystal. Experimental results indicate that grinding intensity and reaction rate have lesser influence on product crystal quality than interruptions of the reaction progress. An inverse dependency of the induction time on the seed crystal quantity in seeded LAG experiments was found. This might be attributed to surface passivation of the seed crystals. The quantitative analysis of the cocrystal mass fraction in seeded LAG experiments may indicate diffusion or dissolving limitation on the reaction velocity.

INTRODUCTION

In developing new high explosives, high performance is a key feature.[1] However, high performance is usually linked to high sensitivity.[2] In accordance with this trend, CL-20 (2,4,6,8,10,12-hexanitro-2,4,6,8,10,12-hexaazaisowurtzitane) surpasses HMX (octahydro-1,3,5,7-tetranitro-1,3,5,7-tetrazocine) in terms of detonation velocity,[1] but shows also a higher sensitivity.[3] Matzger *et al.* created a 2:1 CL-20/HMX cocrystal that combines the higher performance of CL-20 with the lower sensitivity of HMX.[4] There are several methods described in literature for the formation of this cocrystal including spray flash evaporation,[5] liquid assisted grinding (LAG),[4,6] and solution cocrystallization.[6] Bolton *et al.* used seed crystals to convert γ-CL-20 and γ- or α-HMX in 2-propanol within five days into the cocrystal,[4] while Anderson *et al.*

achieved total conversion of CL-20 and HMX in a mixture of acetonitrile and 2-propanol within one hour via resonant acoustic mixing.[6]

Multiple effects in the mechanism of mechanochemical synthesis have been attributed to grinding, such as, creating amorphous phases,[7] refreshing the crystal surfaces,[8,9] and reducing the particle size.[10] While some mechanochemical reactions seem to exhibit an energy threshold, that has to be overcome for a reaction to occure,[8,11] other systems require no cogrinding of reaction partners.[12,13]

Whether or not grinding is essential for the reaction progress, vigorous grinding can be expected to shorten conversion time, at least via reducing the particle diameters, but this procedure might on the other hand be detrimental to product crystal quality. While inducing amorphous phases in educts may be desirable to facilitate the cocrystallization, the potential grinding induced crystal lattice distortion[14] of product crystals is undesirable. In addition, the overall increased reaction speed might also be of disadvantage concerning the product crystal quality, because fast growth increases the probability of inclusions.[15]

In order to examine the influence of grinding on the formation and crystal quality of the CL-20/HMX cocrystal, an experimental set up was designed which allowed for a minimal amount of grinding via the use of a slow rotating paddle agitator. In addition the kinetic of the cocrystallization via LAG was studied.

EXPERIMENTAL SECTION

Solvents

All solvents were reagent grade or higher and dried over 3Å molecular sieve.

Cocrystallization via slow rotating paddle agitator

50 ml 2-propanol was added to ε-CL-20 (30.00 g, 68.46 mmol) and β-HMX (10.14 g, 34.23 mmol). The mixture was stirred via a paddle agitator rotating at 50 rpm at 40°C in a jacketed vessel for 860 h. At this point X-ray diffraction and Rietveld analysis showed a purity of over 99.5%. The agitator was custom made to fit the jacketed vessel and leave a 1 mm gap between agitator and inner wall. The agitator's paddle is 30 mm wide, 80 mm high and exhibits fourteen 5 mm holes in two vertical rows.

The experiment had to be interrupted several times, due to the unanticipated long reaction time.

Kinetic experiment

The experiment was carried out threefold. 4 ml 2-propanol was added to ε-CL-20 (1.600 g, 3.651 mmol) and β-HMX (0.541 g, 1.83 mmol). 0.050 g (**1**), 0.108 g (**2**) and 0,149 g Cl-20/HMX cocrystal (**3**), obtained in the cocrystallization via slow rotating paddle agitator, was added as seed crystals to the reaction mixture **1**, **2**, and **3**, respectively. The reaction vessels are 23 mm in diameter, hold 20 ml, and possess rounded bottoms. Two 3.2 mm and two 4.9 mm glass beads were added as grinding balls. The reaction mixtures were tempered at 40°C und circularly agitated at 1200 rpm via a Ditabis MKR 23 thermo block mixer equipped with a matching thermo block for the reaction vessels. The loaded reaction vessels were allowed to reach 40°C before the agitation was started which also started the reaction timer. 5 µl and 50 µl samples were collected for Raman and particle diameter measurements after 1 h 30 min from all reaction vessels in 10 and 30 minutes intervals, respectively, via syringe through septum. Within two minutes after sample taking, the 2-propanol was removed from the samples via vacuum at 20°C.

Density measurement

The density of the cocrystal prepared via slow rotating paddle agitator was measured by a Quantachrome Ultrapycnometer 1000 version 2.4 using Helium as carrier gas. The cell volume V_C was calibrated prior to every measurement run, consisting of 30 individual measurements. The purge time was 5 minutes and the target pressure was 130 kPa. Flow was chosen as measurement mode. Based on the variance of each run and on the assumption of t-distributed[16] measurement results, a Welch-test[17] with a significance level of 0.05 was carried out to test for statistically significant influences of the measurement conditions. On fulfilling the null hypothesis, the individual density values were pooled and the 95% confidence intervals[18] for the results were determined.

Raman measurements

Raman spectra were collected with a Brucker RFS 100/S Raman spectrometer equipped with a 1064 nm ND:YAG-laser operated at 450 mW and a liquid nitrogen cooled Germanium-detector. The spectra were collected between 80 and 3500 cm^{-1} with a spectral resolution of 1 cm^{-1}. Each spectrum was obtained by summing 150 scans. The quantitative conversion determination was carried out on the basis of a calibration consisting of 10 CL-20/HMX/cocrystal mixtures by comparing the peak integral in the interval from 811.19-824.70 cm^{-1} with the peak integral in the interval from 824.70-848.53 cm^{-1} and by comparing the peak integral in the interval from 2975.00-2997.86 cm^{-1} with the peak integral in the interval from 2997.86-3012.45 cm^{-1}.This procedure was chosen to eliminate possible influences caused by baseline shifts by only comparing neighboring peaks.

Particle diameter measurements

Particle diameters were determined with a Malvern Mastersizer 2000 version 5.60, with a heptane-lecithin mixture as dispersion medium. The agitation speed was 2450 rpm. Prior to every measurement, injected samples were ultrasonicated for 2 minutes with 60% intensity. As refractive index 1.69 and as absorption coefficient 0.001 was chosen. Three measurements each consisting of 10000 individual scans were averaged.

DSC measurement

DSC Measurements were carried out with a TA Instruments DSC Q2000 Version 24.10 Build 122, and a heat rate of 2 K min^{-1}.

FE-SEM measurements

Field emission- scanning electron microscope images were taken by a Zeiss SUPRA 55 VP. The samples were prepared by sputter-coating with Au/Pd (80/20).

XRD

X-ray powder diffraction measurements were performed on a D8 Advance from Bruker AXS, equipped with copper tube, two 2.5° Soller collimators, anti-scatter

screen, flip-stick stage, and silicon strip detector (LynxEye). The data was evaluated using Rietveld analysis based on the structure data reported by Bolton *et al*.[4]

RESULTS AND DISCUSSION

LAG at 40°C agitated via slow rotating paddle agitator

Figure 1 (upper part) shows a representative FE-SEM image of the obtained cocrystal after 860 h reaction time. Some distinct features are apparent in comparison to a representative FE-SEM image of **1** (**Figure 1** lower part). The crystal habitus is less defined and no sharp edges are present. Also, the particles appear stronger intergrown and more pores are observable. The more rounded crystal shape might be the result of the prolonged reaction time. Because of the low conversion rate towards the end of the reaction, fully grown cocrystals were present for several hundred hours of agitation, while almost no further conversion occurred. Therefore, constant, prolonged attrition might have rounded the edges while almost no reconstruction by cocrystallization occurred. The higher degree of intergrowth is likely the result of the low agitation rate, as higher stirrer speeds reduce the aggregation efficiency and increase particle disruption.[19] The higher concentration of pores may be the result of the repeated interruptions of the experiment, because interrupted growth can result in inclusions.[15] During the interruptions the temperature in the reaction vessel usually dropped to around 16 °C and no agitation occurred. Previous results indicate the strong temperature dependency of this cocrystallization,[20] which is why, for all practical purposes, the cocrystallization can be considered interrupted. It appears the lower crystallization velocity compared to the kinetic experiment (about 42 h compared to 5.8h to reach 50% conversion) did not result in an apparent positive effect on the crystal quality.

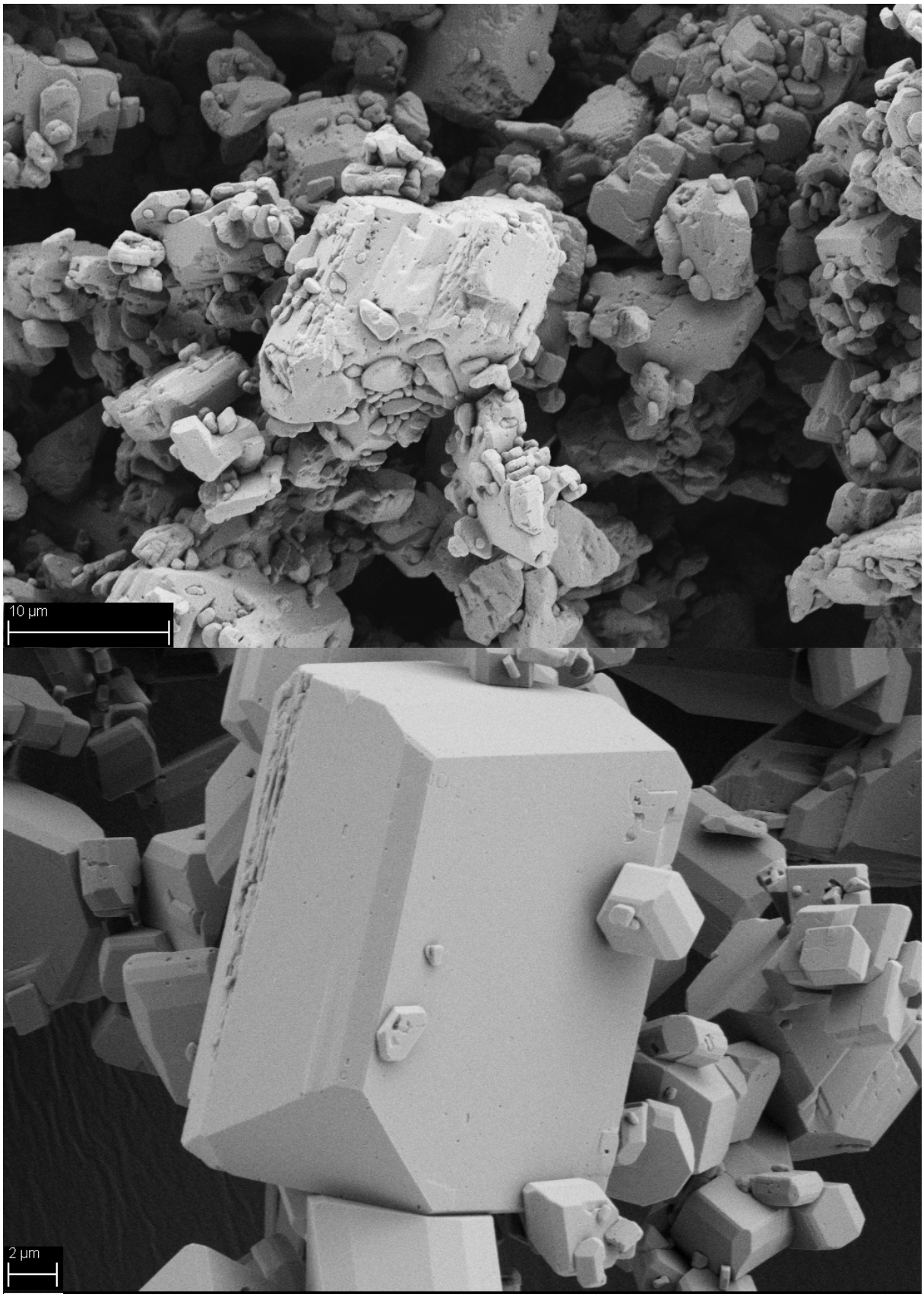

Figure 1:(upper image) FE-SEM image of the CL-20/HMX cocrystal obtained via LAG at 40°C agitated via slow rotating paddle agitator. (lower image) FE-SEM image of **1**.

The received density measurement data are summarized in Table 1. The received pooled density is in good agreement with the previously described crystallographic density of 1.945 $\frac{g}{cm^3}$ at roomtemperature.[4]

Table 1: Summary of the density measurement parameters of the cocrystal obtained via LAG at 40°C agitated via slow rotating paddle agitator. The upper and lower bounds correspond to the 95% confidence intervals. The ultra pycnometer's cell temperature was 21.8°C and 21.9°C for measurement 1 and 2, respectively. The sample mass was 3.2708 g and 3.2142 g for measurement 1 and 2, respectively.

				density [$\frac{g}{cm^3}$]	
	Sample size	variance	Lower bound	Sample mean	Upper bound
Measurement 1	30	2.0818E-06	1.9454	1.9459	1.9465
Measurement 2	30	2.7743E-05	1.9446	1.9466	1.9486
pooled data	60	1.5029E-05	1.9453	1.9463	1.9473

The PXRD pattern (**Figure 2**), the Raman spectrum (**Figure 3**), and the DSC (**Figure 4**) of the CL-20/HMX cocrystal received via LAG at 40°C agitated via slow rotating paddle agitator are in agreement with the previously reported data.[4,5,6]

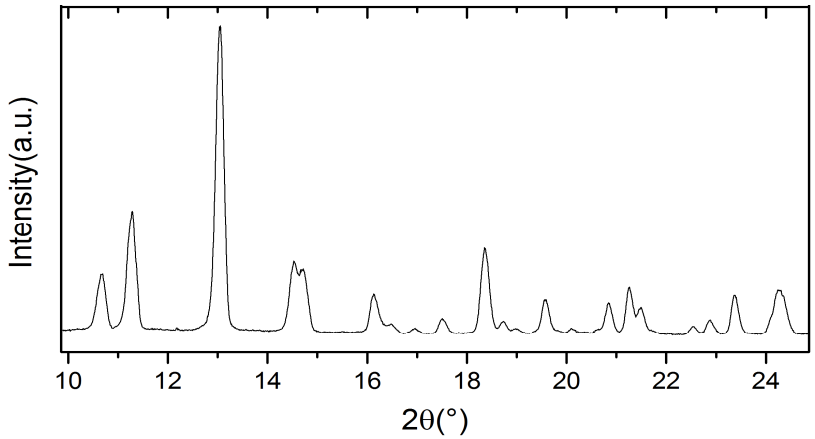

Figure 2: Powder X-ray diffraction pattern of the CL-20/HMX cocrystal obtained via LAG at 40°C agitated via slow rotating paddle agitator.

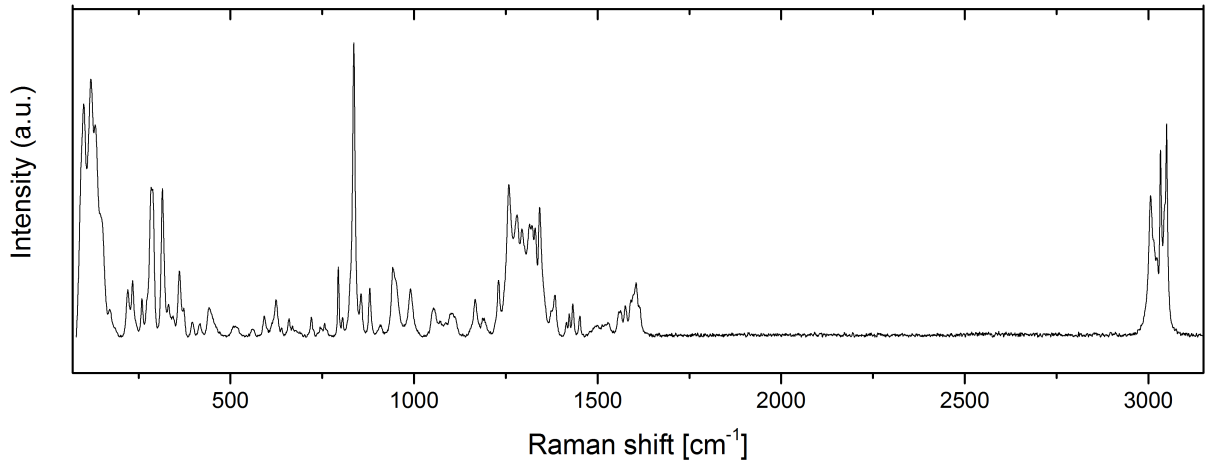

Figure 3: Raman shift of the CL-20/HMX cocrystal obtained via LAG at 40°C agitated via slow rotating paddle agitator.

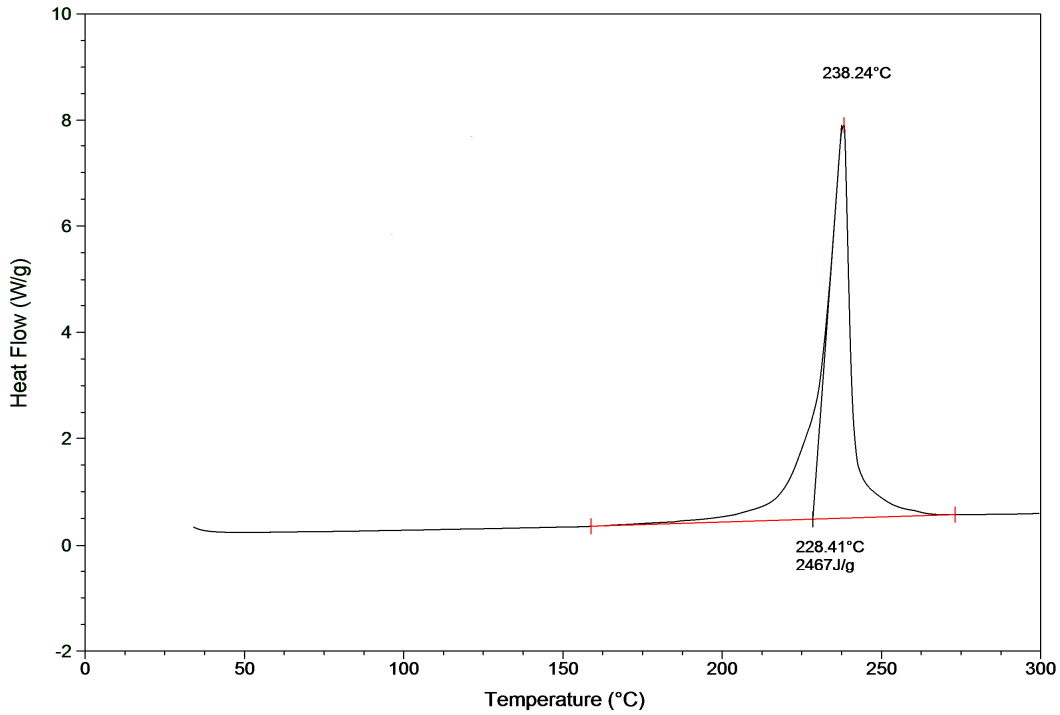

Figure 4: DSC of the CL-20/HMX cocrystal obtained via LAG at 40°C agitated via slow rotating paddle agitator.

The volume weighted mean particle size is 9.2 µm.

Impact and friction sensitivity tests of the CL-20/HMX cocrystal, β-HMX, and ε-CL-20 were carried out in accordance with DIN EN 13631-4 and DIN EN 13631-3. In **Table 2** the received data for the CL-20/HMX cocrystal and the data of the starting materials are compared to previously obtained data.[6,20]

Table 2: Summary of the drop and impact sensitivity of the CL-20/HMX cocrystal, β-HMX, and ε-CL-20.

Material	Impact sensitivity [Nm]	Friction sensitivity [N]
CL-20/HMX cocrystal	2.5, 1.5[20], 4.2[6]	72, 168[20], 72[6]
β-HMX	7.5[20]	144[20]
ε-CL-20	1[20]	108[20]

The obtained friction sensitivity data is identical with the data reported by Anderson *et al.,*[6] while the cocrystal shows higher sensitivity to impact than reported.[4,6] Further experiments are necessary to determine whether the difference to the prior determined sensitivity data[20] is caused by differences in the experimental conditions and the thereby resulting cocrystal properties.

Kinetic experiment

The time dependent mass fraction of the cocrystal for **1**, **2**, and **3** is shown in **Figure 5**. Unfortunately the conversion curves of **2** and **3** are trimmed in the beginning due to the unanticipated short induction time. The overall shapes of the

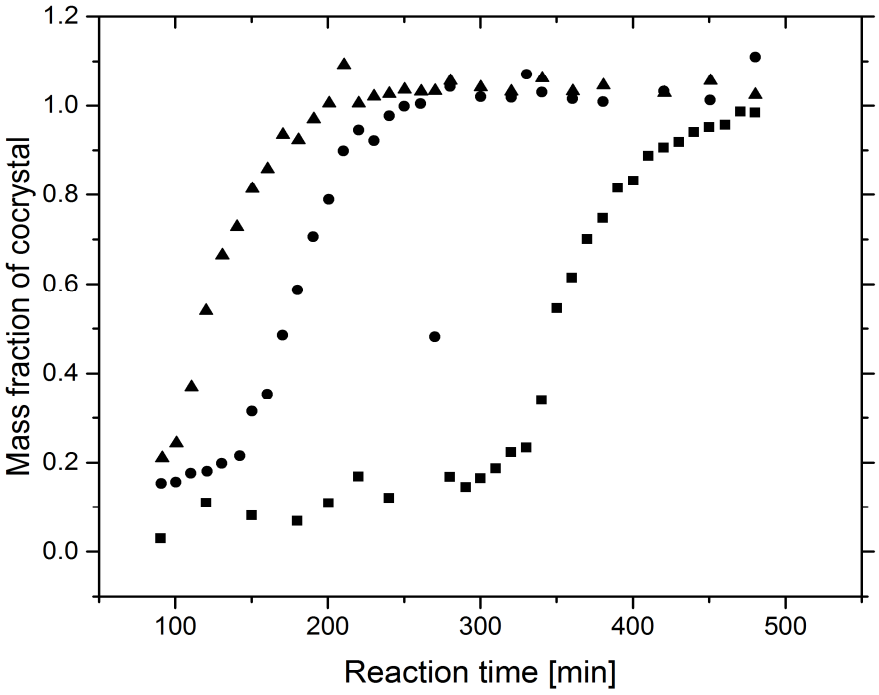

Figure 5: The time dependent mass fraction of the cocrystal for **1** (squares), **2** (circles), and **3** (triangles).

conversion curves appear to be sigmoidal. In order to investigate the kinetic of this cocrystallization, the time dependent cocrystal mass fraction was fitted to ten reaction

models[21,22]: By utilizing a double logarithmic plot, a generalized power law and Avrami-Erofe'ev form was achieved in which the slope of the linear fit corresponds to the reciprocal value of the respective power. Furthermore the Prout-Tompkins (B1), the geometrical contraction models (R2) and (R3), the diffusion models (D1), (D2), (D3), and (D4), and first-order model (F1) were fitted. No satisfying fits were accomplished for **1** and **2**. This is due to the fact that the time dependent cocrystal mass fraction shows a linear increase up to 0.2, after which a steep increase of the conversion rate seems to appear. One possible explanation for this behavior is that the cocrystallization changes its kinetic at this point. Plotting the induction period as a function of the added seed crystal mass indicates an inverse dependence between seed crystal mass and induction time (**Figure 6**). A similar dependency was found by Hook[23] and Davies *et al*[24] for the crystallization of silver chromate and silver chloride, respectively. Davies *et al.* found that at the beginning of the induction period a passivating adsorption layer covered the seed crystal surface, which is then continuously removed via desorption.[24] The possible surface contamination of the cocrystal, obtained via LAG at 40°C agitated via slow rotating paddle agitator, which was used as seed crystals, might have occurred in the process of the cocrystallization. Because of the long reaction time at 40°C traces of decomposition product possibly were generated and adsorbed to the surface. One point that might contradict the involvement of surface contamination in the varying induction time is the constant and intense grinding of the reaction mixture during the reaction. This grinding might be sufficient to remove a minor surface contamination rather quickly, and, therefore, there should not have been an induction period observable. It is, however, also possible that only because of the vigorous grinding a slow refreshing of the seed crystals occurred. It should, furthermore, be noted that no contamination is visible in the Raman spectrum.

The time dependent cocrystal mass fraction was fitted again to the ten reaction models in the interval from 0.2 to 0.99. The received coefficients of determination (R^2) summarized in **Table 3** estimate the fit qualities.

Table 3: Coefficients of determination of kinetic fits.

model	**1**	**2**	**3**
Generalized power law	0.77	0.90	0.91
Generalized Avrami-Erofe'ev	0.93	0.98	0.98
B1	0.98	0.85	0.99
R2	0.96	0.98	0.99
R3	0.98	0.97	0.99
D1	0.93	0.96	0.98
D2	0.98	0.97	0.98
D3	0.97	0.86	0.92
D4	0.99	0.96	0.97
F1	0.97	0.76	0.96

The significant amount of seed crystals should prevent the cocrystallization from being nucleation controlled. Therefore, the power law, Avrami-Erofe'ev, and B1 models should not fit the received data well. It is, however, evident from **Table 3** that none of the models describes all three time dependent cocrystal mass fractions well. One factor in the unsatisfying fit, of course, is the coarseness of the data, as well as the relatively long time intervals between measurements. Another factor is that the reaction involves multiple substances (CL-20 and HMX), including a liquid (2-propanol), and thereby diverges from classical solid-state reactivity models. A final point to consider is that the reaction appears to proceed linearly in the cocrystal mass fraction interval from 0.0 to 0.2, and, therefore, a superposition of two competing kinetic dependencies might be present. This superposition might be the result of the surface passivation of the added seed crystals, thereby enable nucleation to occur in the beginning. Even though the model fits do not yield solid kinetic information, the slopes of the conversions might indicate to solubility related control. For **1**, **2**, and **3** the conversion of the mass fraction of cocrystal from 0.2 to 0.8 occurs within 6 to 7 data points being equivalent to a time interval of about one hour. Van Hook found an increase in the overall velocity of the crystallization of silver chromate by progressive addition of seed crystals, in addition to the shortening of the induction period.[23] This behavior can be expected for initially passivated seed crystals, if the reaction is controlled by the crystal growth speed. In the case of **1**, **2**, and **3** however, an increase of the seed crystal mass did not increase the maximum reaction velocity, which might indicate that the reaction is either controlled by diffusion in the solvent or by the dissolving of the educts.

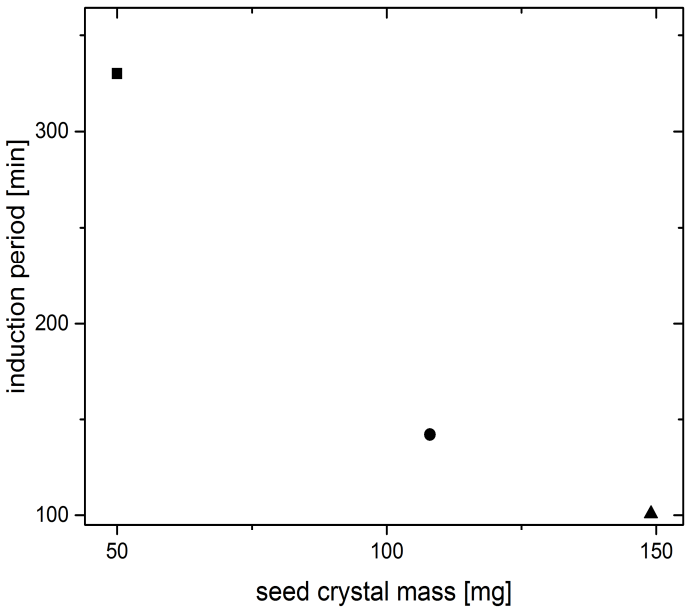

Figure 6: Induction period as a function of the seed crystal mass of **1**(square), **2**(circle) and **3**(triangle).

The comparison of the received particle sizes might indicate that the added cocrystal acted as seed crystals, because **1**, **2** and **3** exhibit a volume weighted particle size distribution of overall larger particles than the seed crystals (**Figure 7**). In addition **1**

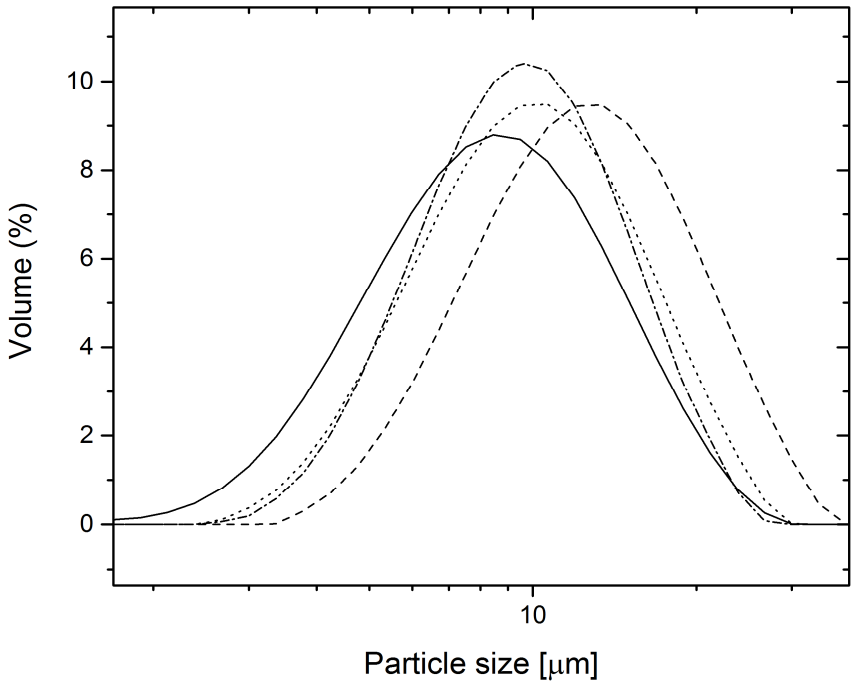

Figure 7: Volume weighted mean particle size of **1**(dashed line), **2**(dotted line), **3**(dashed and dotted line), and seed crystals (continuous line) at 99%, 100%, 100%, and 100% conversion, respectively.

consists of larger particles than **2** and **3**, and **2** exhibits a slightly larger average volume weighted particle size than **3**, possibly as a result of the smaller number of seed crystals in **1** compared to **2**, and in **2** compared to **3**, which lead to growth of larger crystals in **1** compared to **2**, and **2** compared to **3**.

CONCLUSION

The received cocrystal quality of CL-20 and HMX generated via LAG appears to be rather dependent on the interruption of the crystallization and less dependent on the crystallization velocity and grinding intensity. Long exposure of the cocrystal at 40°C to 2-propanol might lead to a surface passivation by unknown material which leads to an induction period in seeded LAG cocrystallizations with an inverse induction time dependency on the seed crystal amount. Furthermore, the kinetic data might indicate diffusion or dissolving limitation on the reaction velocity once the induction period is over.

ACKNOWLEDGEMENT

We are grateful for financial support provided by the German Ministry of Defense and the support provided by Dr. Manfred Kaiser at the WTD91.

[1] J. P. Agrawal, *Prop., Explos., Pyrotech.* **2005***, 30*, No. 5, 316
[2] a)P. Politzer, J. S. Murray, *J. Mol. Model* **2015**, *21*, 25
b) C. Zhang, Y. Cao, H. Li, Y. Zhou, J. Zhou, T. Gao, H. Zhang, Z. Yang, G. Jiang, *Cryst. Eng. Comm.* **2013**, *15*, 4003
[3] R. L. Simpson, P. A. Urtiew, D. L. Ornellas, G. L. Moody, K. J. Scribner, D. M. Hoffman, *Prop., Explos., Pyrotech.* **1997**, *22*, No. 5, 249
[4] O. Bolton, L. R. Simke, P. F. Pagoria, A. J. Matzger, *Cryst. Growth Des.* **2012**, *12*, 4311
[5] a) D. Spitzer, B. Risse, F. Schnell, V. Pichot, M. Klaumünzer, M. R. Schaefer, *Sci. Rep.* **2014**, *4*, 6575
b) B. Gao, D. Wang, J. Zhang, Y. Hu, J. Shen, J. Wang, B. Huang, Z. Qiao, H. Huang, F. Nie, G. Yang, *J. Mater. Chem. A* **2014**, *2*, 19969
[6] S. R. Anderson, D. J. am Ende, J. S. Salan, P. Samuels, *Prop., Explos., Pyrotech*. **2014**, *39*, No. 5, 637
[7] K. Seefeldt, J. Miller, F. Alvarez-Núñez, N. Rodríguez-Hornedo, *J. Pharm. Sci.* **2007**, *96*, 5, 1147-1158
[8] R. Kuroda, K. Higashiguchi, S. Hasebe, Y. Imai, *CrystEngComm* **2004**, *6*, 76, 463-468
[9] G. Kaupp, *Cryst. Eng. Comm.* **2003**, *5*, 23, 117-133
[10] G. A. Bowmaker, J. V. Hanna, R. D. Hart, B. W. Skeleton, A. H. White, *Dalton Trans.* **2008**, 5290-5292
[11] R. Kuroda, Y. Imai, N. Tajima, *Chem. Commun.* **2002**, 2848-2849
[12] R. P. Rastogi, P. S. Bassi, S. L. Chadha, *J. Phys. Chem.* **1962**, *66*, 2707-2708
[13] G. A. Bowmaker, J. V. Hanna, B. W. Skelton, A. H. White, *Chem. Commun*. **2009**, 2168-2170
[14] F. P. A. Fabbiani, C. R. Pulham, *Chem. Soc. Rev.* **2006**, *35*, 932-942

[15] J. W. Mullin, *Crystallization*, Oxford: Butterworth-Heinemann, 2001, print
[16] Student (a.k.a W. S. Gosset), *Biometrica* **1908**, *6*, 1, 1-25
[17] B. L. Welch, *Biometrica* **1947**, 28-35
[18] Konfidenz J. Neyman, Philos. *T. R. Soc. A* **1937**, *236*, 767, 334-380
[19] R. Zauner, A. G. Jones, *Chem. Eng. Sci.* **2000**, *55*, 4219-4232
[20] D. Herrmannsdörfer, M. Herrmann, T. Heinz, *46th international annual conference of the Fraunhofer ICT*, June 23-26, Karlsruhe, Germany, **2015**, 107.1-107.9
[21] A. Khawam, D. R. Flanagan, *J. Phys. Chem. B* **2006**, *110*, 35, 17315-17328
[22] A. Khawam, D. R. Flanagan, *J. Pharm. Sci.* **2006**, *95*, 3, 472-498
[23] A. van Hook, *J. Phys Chem.* **1940**, *44*, 751-765
[24] C. W. Davies, A. L. Jones, G. H. Nancollas, *Trans. Faraday. Soc.* **1955**, *51*, 1232-1234